Synthesis of bamboo-shaped carbon–nitrogen nanotubes using C_2H_2–NH_3–$Fe(CO)_5$ system

Cheol Jin Lee [a,*], Seung Chul Lyu [a], Hyoun-Woo Kim [b], Jin Ho Lee [c], Kyoung Ik Cho [c]

[a] *Department of Nanotechnology, Hanyang University, 17 Haengdang-dong, Seongdong-gu, Seoul 133-791, Republic of Korea*
[b] *School of Materials Science and Engineering, Inha University, Inchon 402-751, Republic of Korea*
[c] *Microelectronics Labs, Next Generation Semiconductor Research Department of ETRI, Taejon 305-350, Republic of Korea*

Abstract

Aligned bamboo-shaped carbon–nitrogen nanotubes have been massively produced by the pyrolysis of iron pentacarbonyl ($Fe(CO)_5$) and acetylene (C_2H_2) mixtures with ammonia (NH_3) being the source of nitrogen. With nitrogen doping, the nanotubes have a bamboo-like structure and reveal degraded crystallinity of graphite sheets. Nitrogen plays a key role in generating compartment layers inside the nanotube. A base-growth model is adequate to explain the carbon–nitrogen nanotube growth. © 2002 Elsevier Science B.V. All rights reserved.

1. Introduction

Since the first observation by Iijima [1], carbon nanotubes have attracted much interest due to their novel electronic and mechanical properties [2–4]. Carbon nanotubes have numerous potential applications such as flat panel displays [5], vehicles for large hydrogen storage [6], chemical sensors [7], and nanoscale electronic devices [8].

Recently, some research groups predicted that carbon nitrides are superhard and metallic in comparison with pure carbon structures [9,10]. Accordingly, many researchers have been inter-ested in the synthesis of carbon–nitrogen (CN) nanotubes, with an expectation to improve the nanotube properties.

Although many research groups have reported on the CN nanotube growth by various methods such as magnetron sputtering [11], chemical vapor deposition (CVD) [12–14], and pyrolysis [15–20], there were not many systematic studies on the structure and crystallinity of CN nanotubes.

In this Letter, we report a large-scale synthesis of CN nanotubes using the reaction gases (C_2H_2 and NH_3) and the catalyst source ($Fe(CO)_5$) in a single-furnace quartz reactor at the temperature range of 750–950 °C. We also investigate the structure and crystallinity of CN nanotubes in comparison with those of carbon nanotubes by transmission electron microscopy (TEM),

---

* Corresponding author.
E-mail address: cjlee@hanyang.ac.kr (C.J. Lee).

thermogravimetric analysis (TGA), and Raman spectroscopy. Based on TEM observation, we suggest a growth mechanism of CN nanotubes.

2. Experimental

The apparatus for vapor phase growth consists of a horizontal quartz tube with an inner diameter of 20 mm and a heating zone of 200 mm. Previous studies reveal that the iron particle is an efficient catalyst for synthesizing carbon nanotubes [21,22]. To supply a iron catalyst source into the reactor, C_2H_2 gas was flowed through the liquid $Fe(CO)_5$ bubbler which was maintained at room temperature. The reaction gases (C_2H_2, NH_3) and the carrier gas (Ar) were directly introduced into the reactor. The flow rates of C_2H_2, NH_3, and Ar were 20, 30, and 1500 sccm, respectively. A high-flow rate of Ar carrier gas was used for even distribution of the catalyst within a quartz tube [23]. The synthesis temperature ranged from 750 to 950 °C for 30 min. After the reaction, Ar carrier gas with the flow rate of 500 sccm was flowed into the reactor while cooling down to room temperature. In order to compare CN nanotubes with carbon nanotubes, the carbon nanotubes were synthesized at the same condition without flowing NH_3 gas.

A scanning electron microscope (SEM) (Hitachi S-800, 30 kV) was used to measure the length and diameter of nanotubes. A TEM (Philips, CM20T, 200 kV) was used to investigate the structure and crystallinity of nanotubes, with the deposits separated from the quartz tube and dispersed on a carbon TEM microgrid. A Raman spectrometer (Renishaw micro-Raman 2000) and a TGA (SDT 2960, TA instrument) were used to evaluate the overall crystallinity of nanotubes. The stoichiometry of the carbon and nitrogen atoms in the nanotubes were examined by X-ray photoelectron spectroscopy (XPS) (VG scientific ESCA LAB).

3. Results and discussion

A dense film was deposited homogeneously along the total heating zone inside the quartz reactor at all temperatures in the range of 750–950 °C. Figs. 1a–c show SEM micrographs of nanotubes synthesized with NH_3 at 750–950 °C. The average lengths of nanotubes are about 24, 26, and 30 μm, respectively, at 750, 850, and 950 °C. To evaluate the nitrogen doping effect on the growth of nanotubes, we synthesized nanotubes at the same condition without NH_3 gas. Figs. 1d–f show SEM micrographs of nanotubes synthesized
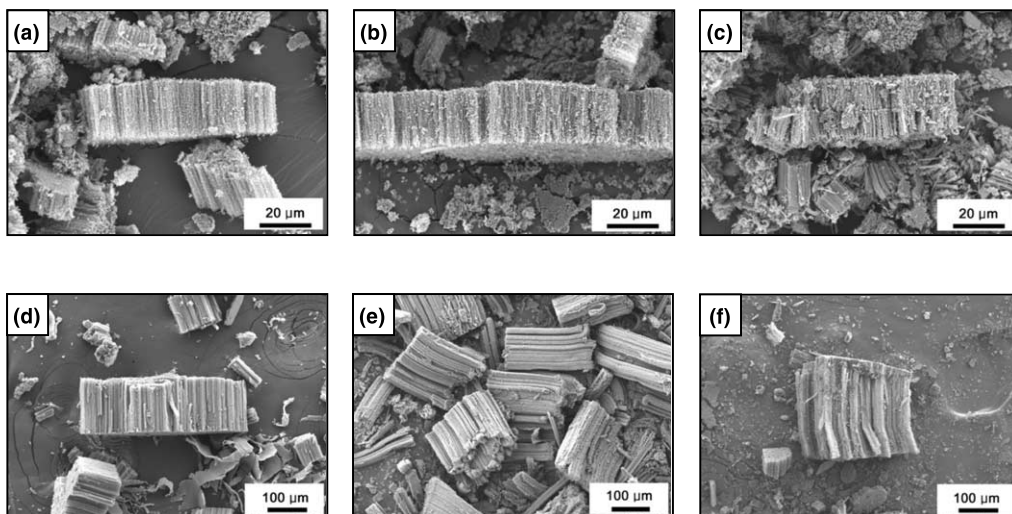

Fig. 1. SEM micrographs of nanotubes synthesized at 750–950 °C with 20 sccm of C_2H_2, 1500 sccm of Ar. Nanotubes synthesized with NH_3 (a) at 750 °C, (b) at 850 °C, and (c) at 950 °C, without NH_3 (d) at 750 °C, (e) at 850 °C, and (f) at 950 °C, respectively.

without NH_3. The average lengths of nanotubes are about 140, 220, and 280 μm, respectively, at 750, 850, and 950 °C. By adding NH_3 gas, the growth rate of nanotubes decreases regardless of the growth temperature. The diameters of nanotubes synthesized with NH_3 are about 30, 35, and 37 nm, respectively, at 750, 850, and 950 °C. The diameter of nanotubes slightly increases with increasing growth temperature in the range of 750–950 °C. As the growth temperature increases, more agglomeration occurs at a higher temperature, resulting in a larger sized catalyst with low density.

XPS analysis shows that the nanotubes consist of carbon accompanied by traces of nitrogen. In Fig. 2a, XPS spectrum shows that the C1s signal is at 285 eV and the N 1s signal is at around 400 eV [18]. We estimated the ratio of carbon to nitrogen by taking the ratio of the integrated peak areas under the C 1s and N 1s signal (without spectral decomposition) and dividing them by the respective photoionization cross sections. Fig. 2b shows the average concentration of nitrogen at the nanotubes according to the growth temperature. The nitrogen concentrations of nanotubes (atomic percent) grown at 750, 850, and 950 °C are 2.8%, 4.2%, and 6.6%, respectively, and their compositions are about $C_{36}N$, $C_{24}N$, and $C_{15}N$. The nitrogen concentration of nanotubes increases with increasing growth temperature. In our experiments, the incorporation of nitrogen into nanotubes was clearly confirmed by adding NH_3 gas and this result agrees with a previous study [20].

To investigate the structure and crystallinity of nanotubes according to nitrogen doping, we analyzed TEM images of CN nanotubes (Figs. 3a–d) and carbon nanotubes (Figs. 3e and f) simultaneously. Fig. 3a shows TEM images of CN nanotubes synthesized at 850 °C. The high-purity CN nanotubes without carbonaceous particles are grown on the inner surface of the quartz tube, although some metal catalyst particles are included inside the tubes. The CN nanotubes reveal hollow inside and the outer diameter of the CN nanotubes is almost constant over a long distance. Fig. 3b shows that CN nanotubes have a bamboo-like structure with compartment layers. The closed tip of a CN nanotube is shown in Fig. 3c. A high-resolution TEM (HRTEM) image of a CN nanotube
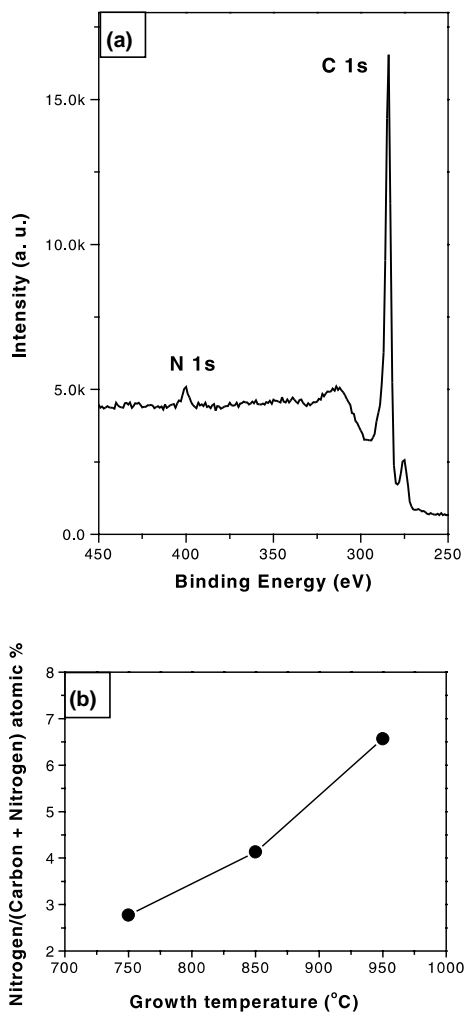

Fig. 2. XPS analysis of CN nanotubes. (a) XPS spectrum of C and N elements. (b) Nitrogen concentration of CN nanotubes according to the growth temperature. The average composition of CN nanotubes synthesized at 750, 850, and 950 °C are about $C_{36}N$, $C_{24}N$, and $C_{15}N$, respectively.

indicates defective graphite sheets with waving morphology (Fig. 3d). In general, the waving morphology of graphite sheets is from a defective structure, caused by the appearance of pentagons and hexagons instead of hexagons [24]. In our experiments, all the CN nanotubes reveal a bamboo-like structure and corrugated graphite sheets regardless of growth temperature in the range of 750–950 °C. Fig. 3e shows a TEM image of carbon nanotubes without nitrogen doping, showing rare
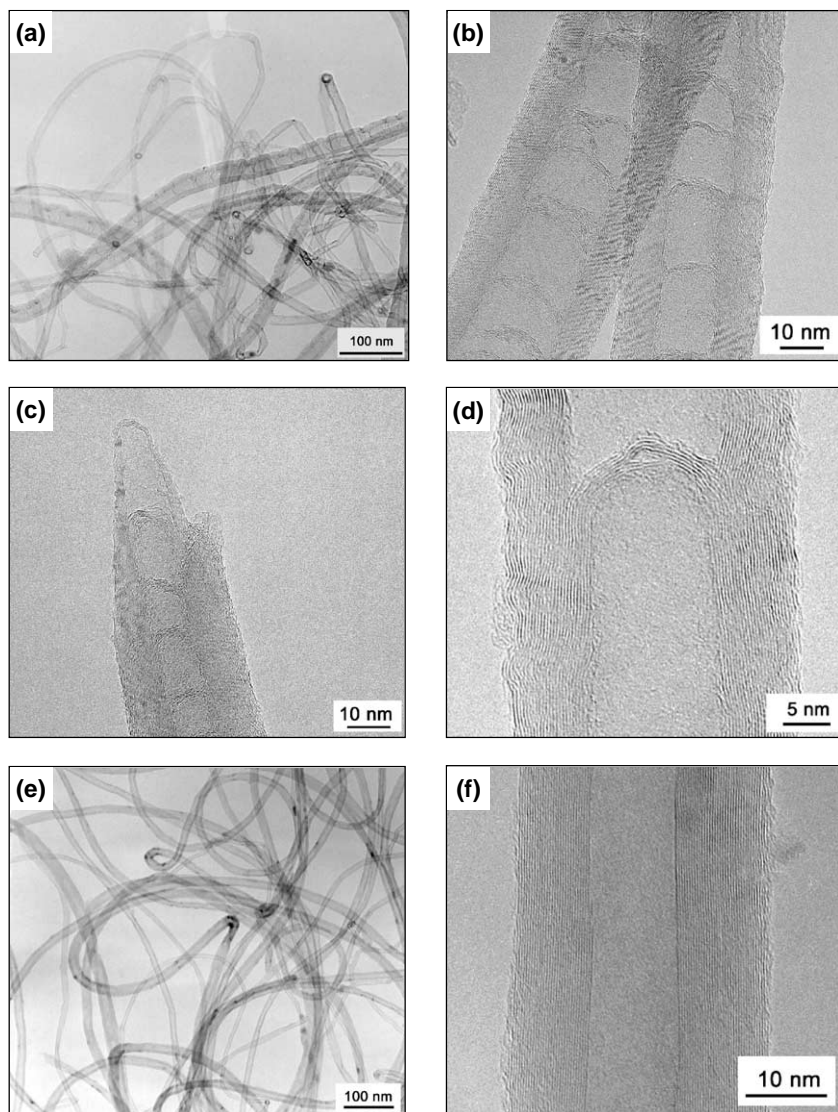
Fig. 3. TEM images of nanotubes synthesized at 850 °C. (a)–(d) With nitrogen doping. (e)–(f) Without nitrogen doping. (a) Low magnification TEM image of CN nanotubes. (b) The CN nanotubes showing a bamboo-like structure with compartment layers. (c) A closed tip of a CN nanotube. (d) HRTEM image of a CN nanotube, revealing defective graphite sheets. (e) Low magnification TEM image of carbon nanotubes. (f) HRTEM image of a carbon nanotube, revealing straight graphite fringes.

compartment layers. Fig. 3f shows a HRTEM image of a carbon nanotube, revealing that graphite sheets have straight fringes without waving morphology. It means that the CN nanotubes have more defective structures than carbon nanotubes.

TGA analysis is carried out to obtain the overall information on the crystalline perfection of

nanotubes synthesized at 850 °C. Fig. 4 shows a plot for weight loss in percentage vs. oxidation temperature, measured by heating up the nanotubes in the air ambience. The percentage weight loss curve between 200 and 800 °C is plotted by adjusting 100% for the weight loss at 800 °C, which is presumably the weight of catalyst (usually 10%
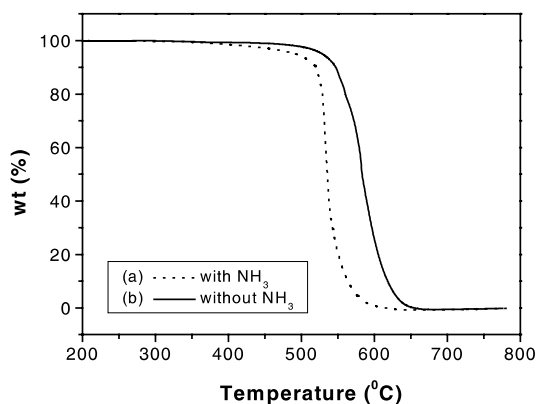
Fig. 4. TGA data of weight loss in percentage vs. oxidation temperature for the nanotubes grown at 850 °C. The nanotubes (a) with and (b) without nitrogen doping start to gasify at 370 and 450 °C, respectively.
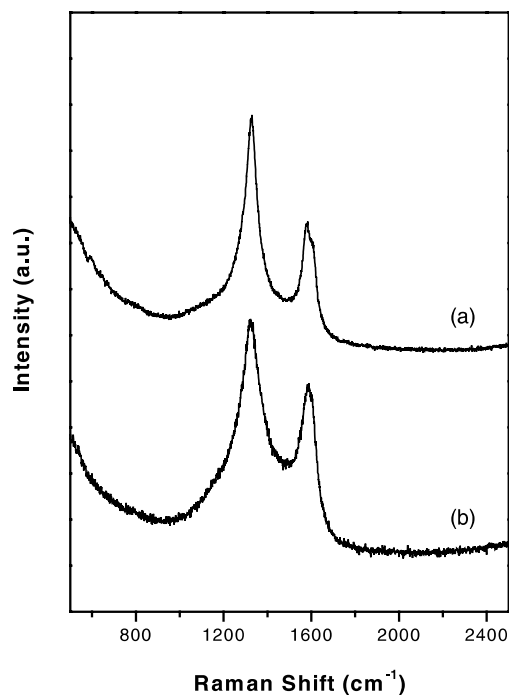

Fig. 5. Raman spectra of nanotubes (a) with and (b) without nitrogen doping. The relative peak intensity of D and G bands increases with nitrogen doping.

of total weight). The CN nanotubes start to gasify at a lower temperature (370 °C) compared with the carbon nanotubes, which burn at 450 °C. It is consistent with HRTEM images, revealing that the crystallinity of nanotubes degrades with nitrogen doping.

Fig. 5 shows Raman spectra of nanotubes grown at 850 °C with and without nitrogen doping. All spectra show mainly two Raman bands at ~1335 cm^{-1} (D band) and ~1580 cm^{-1} (G band). The D band indicates the defective structure of graphite sheets [25]. The peak intensity ratio of D and G bands increases with nitrogen doping, indicating that the crystallinity of CN nanotubes is lower than that of carbon nanotubes. The result of Raman spectra agrees strongly with HRTEM images and TGA data.

We investigated TEM images to explain a growth mechanism of CN nanotubes. Fig. 3b indicates that CN nanotubes consist of hollow compartments, similar to a bamboo-like structure. Fig. 3c shows that a CN nanotube has compartment layers with a curvature directed toward the closed tip which has no encapsulated catalyst particle. In Figs. 3b and d, the wall thickness increases due to the generation of compartment layers, but the outer diameter remains constant. From TEM observation, we suggest that the growth of CN nanotubes follows a base-growth mechanism [26].

The formation of compartment layers caused by nitrogen was observed in previous studies [14,18,19]. In our experiment, it is clear that nitrogen plays an important role in generating compartment layers during the nanotube growth. By adding NH$_3$, the nitrogen adsorbed on the surface of the catalyst particle restrains the surface diffusion of carbon. As a result, the wall growth, due to surface diffusion, is reduced and thus, the growth rate of CN nanotubes decreases compared with carbon nanotubes. On the other hand, by adding NH$_3$, the bulk diffusion of carbon increases relatively. Accordingly, the carbon accumulation at the inner surface of the catalyst particle is enhanced, resulting in the formation of compartment layers.

In summary, CN nanotubes are synthesized massively on the inner surface of the quartz tube by the catalytic reaction of C$_2$H$_2$, NH$_3$, and Fe(CO)$_5$ mixtures at 750–950 °C. The compositions of CN nanotubes synthesized at 750, 850, and 950 °C, respectively, are about C$_{36}$N, C$_{24}$N,

and $C_{15}N$. With nitrogen doping, the growth rate of nanotubes decreases and the crystallinity of nanotubes is degraded. The CN nanotubes have a bamboo-like structure with waving morphology. The nitrogen plays a crucial role in generating a compartment layer. A base-growth model is suitable to explain the growth of CN nanotubes.

Acknowledgements

References

[1] S. Iijima, Nature 354 (1991) 56.
[2] T.M. Whitney, J.S. Jiang, P.C. Searson, C.L. Chien, Science 261 (1993) 1316.
[3] M.M.J. Treacy, T.W. Ebbenson, J.M. Gibson, Nature 381 (1996) 678.
[4] P. Delaney, H.J. Choi, J. Ihm, S.G. Louie, M.L. Cohen, Nature 391 (1998) 466.
[5] W.B. Choi, Y.W. Jin, H.Y. Kim, S.J. Lee, M.J. Yun, J.H. Kang, Y.S. Choi, N.S. Park, N.S. Lee, J.M. Kim, Appl. Phys. Lett. 78 (2001) 1547.
[6] C. Liu, Y.Y. Fan, M. Liu, H.T. Cong, H.M. Cheng, M.S. Dresselhaus, Science 286 (1999) 1127.
[7] J. Kong, N.R. Franklin, C. Zhou, M.G. Chapline, S. Peng, K. Cho, H. Dai, Science 287 (2000) 622.
[8] P.G. Collins, A. Zettl, H. Bando, A. Thess, R.E. Smalley, Science 278 (1997) 100.
[9] D.M. Teter, R.J. Hemley, Science 271 (1996) 53.
[10] Y. Miyamoto, M.L. Cohen, S.G. Louie, Solid State Commun. 102 (1997) 605.
[11] K. Suenaga, M.P. Johansson, N. Hellgren, E. Broitman, L.R. Wallenberg, C. Colliex, J.-E. Sundgren, L. Hultman, Chem. Phys. Lett. 300 (1999) 695.
[12] M. Yudasaka, R. Kikuchi, Y. Ohki, S. Yoshimura, Carbon 35 (1997) 195.
[13] S.L. Sung, S.H. Tsai, C.H. Tseng, F.K. Chiang, X.W. Liu, H.C. Shih, Appl. Phys. Lett. 74 (1999) 197.
[14] X. Ma, E.G. Wang, Appl. Phys. Lett. 78 (2001) 978.
[15] M. Terrones, N. Grobert, J.P. Zhang, H. Terrones, J. Olivares, W.K. Hsu, J.P. Hare, A.K. Cheetham, H.W. Kroto, D.R.M. Walton, Chem. Phys. Lett. 285 (1998) 299.
[16] M. Terrones, P. Redlich, N. Crobert, S. Trasobares, W.-K. Hsu, H. Terrones, Y.-Q. Zhu, J.P. Hare, C.L. Reeves, A.K. Cheetham, M. Rühle, H.W. Kroto, D.R.M. Walton, Adv. Mater. 11 (1999) 655.
[17] R. Sen, B.C. Satishkumar, A. Govindaraj, K.R. Harikumar, G. Raina, J.-P. Zhang, A.K. Cheetham, C.N.R. Rao, Chem. Phys. Lett. 287 (1998) 671.
[18] M. Nath, B.C. Satishkumar, A. Govindaraj, C.P. Vinod, C.N.R. Rao, Chem. Phys. Lett. 322 (2000) 333.
[19] M. Terrones, H. Terrones, N. Grobert, W.K. Hsu, Y.Q. Zhu, J.P. Hare, H.W. Kroto, D.R.M. Walton, P.K. Redlich, M. Rühle, J.P. Zhang, A.K. Cheetham, Appl. Phys. Lett. 75 (1999) 3932.
[20] W.-Q. Han, P.K. Redlich, T. Seeger, F. Emst, M. Rühle, N. Grobert, W.-K. Hsu, B.-H. Chang, Y.-Q. Zhu, H.W. Kroto, D.R.M. Walton, M. Terrones, H. Terrones, Appl. Phys. Lett. 77 (2000) 1807.
[21] R. Sen, A. Govindaraj, C.N.R. Rao, Chem. Mater. 9 (1997) 2078.
[22] B.C. Satishkumar, A. Govindaraj, C.N.R. Rao, Chem. Phys. Lett. 307 (1999) 158.
[23] M. Mayne, N. Grobert, M. Terrones, R. Kamalakaran, M. Rühle, H.W. Kroto, D.R.M. Walton, Chem. Phys. Lett. 338 (2001) 101.
[24] C.J. Lee, J. Park, Y. Huh, J.Y. Lee, Chem. Phys. Lett. 343 (2001) 33.
[25] F. Tuinstra, J.L. Koenig, J. Chem. Phys. 53 (1970) 1126.
[26] C.J. Lee, J. Park, J. Phys. Chem. B 105 (2001) 2365.